Phase transitions and optimal transport in stochastic roundabout traffic

M. Ebrahim Foulaadvand[1,2,*] and Philipp Maass[3,†]

[1]*Department of Physics, University of Zanjan, P.O. Box 45196-313, Zanjan, Iran*

[2]*School of Nanosciences, Institute for Research in Fundamental Sciences (IPM), Tehran 19395-5531, Iran*

[3]*Fachbereich Physik, Universität Osnabrück, Barbarastraße 7, 49076 Osnabrück, Germany*

(Received 18 February 2016; revised manuscript received 5 June 2016; published 8 July 2016)

We study traffic in a roundabout model, where the dynamics along the interior lane of the roundabout are described by the totally asymmetric simple exclusion process (TASEP). Vehicles can enter the interior lane or exit from it via S intersecting streets with given rates, and locally modified dynamics at the junctions take into account that collisions of entering vehicles with vehicles approaching the entrance point from the interior lane should be avoided. A route matrix specifies the probabilities for vehicles to arrive from and to exit to certain intersecting streets. By subdividing the interior lane into segments between consecutive intersecting streets with effective entrance and exit rates, a classification of the stationary roundabout traffic in terms of TASEP multiphases is given, where each segment can be in either the low-density, high-density, or maximum current TASEP phase. A general methodology is developed, which allows one to calculate the multiphases and optimal throughput conditions based on a mean-field treatment. Explicit analytical results from this treatment are derived for equivalent interesting streets. The results are shown to be in good agreement with kinetic Monte Carlo simulations.

DOI: 10.1103/PhysRevE.94.012304

I. INTRODUCTION

Traffic problems have become an intense interdisciplinary research field because of their widespread relevance in the natural, social, and engineering sciences [1]. In the physics community, knowledge from the areas of nonlinear dynamics, stochastic processes, and statistical physics has been successfully exploited in the past to make important contributions to the basic understanding of conditions for optimal transport and phenomena like jamming, laning, and other collective flow patterns.

Many studies have been carried out to model city traffic and to develop concepts for optimization and controlling [2–12]. Special attention has been paid to single intersections as key elements in the city traffic [13–32]. While signalized intersections are standard for congested traffic, unsignalized intersections become often preferable for less dense traffic. A simple regulation rule in the latter case is that a vehicle farther apart from the intersection point at one lane must give way to a vehicle closer to the intersection point at another lane. Consequences of such rules have been studied in Refs. [33–40]. Elements connecting a number of single intersections are roundabouts, which are nowadays widely used in many countries and are often considered as an alternative for controlling by traffic lights. Their possible benefits have been investigated in Refs. [41–53].

In this work we will study stochastic motion of particles along a roundabout, which contains intersections from where the particles are entering and to which they are exiting. The problem is formulated in terms of vehicular traffic and accordingly we will consider the particles to represent cars. It is, however, not our aim here to set up a detailed modeling of car traffic in a roundabout. Along the interior circulating lane of the roundabout, we model the particle motion by the totally asymmetric exclusion process (TASEP) with stochastic sequential update [54,55]. While this process can give some basic insight into the dynamics, e.g., into the origin of jams, its variant with parallel update would give a modeling closer to reality [1]. Even this variant, although frequently used, is, of course, a strongly simplified description of real car dynamics. The reference to vehicular traffic should be understood here as a paradigm for interfering traffic flows of particles with specified destinations. In this respect our study can provide insights and a methodological basis for treating traffic also in other areas, as, for example, to describe the spread of information packages along communication lines, or the collective transport in networks of microfluidic channels.

An advantage of the TASEP with stochastic sequential update is that analytical treatments are possible, in particular for identifying phases of nonequilibrium steady states. Based on this phase identification, conditions for optimal transport can be derived. The standard TASEP with open boundary condition, i.e., when connected to two reservoirs from and to which particles are injected and ejected, exhibits three different phases [54,55]. These are characterized by the bulk density forming in the system's interior far from the reservoirs and are referred to as the low-density, the high-density, and the maximum current phase.

In our roundabout problem we consider the cars to follow a certain route. This mediates a coupling between the interior parts of the roundabout lane, which depends on details of the junctions connecting the roundabout lane with the intersecting streets. We show that the coupling leads to a rich phase structure in stationary roundabouts, where combinations of different TASEP phases appear. A mean-field treatment is presented that allows one to calculate the phase structure to a good approximation in dependence of the control parameters of the model. Knowing the phase structure, parameter sets can be determined, which give the optimal throughput of cars in the roundabout under different external conditions.

*foolad@iasbs.ac.ir

†maass@uos.de

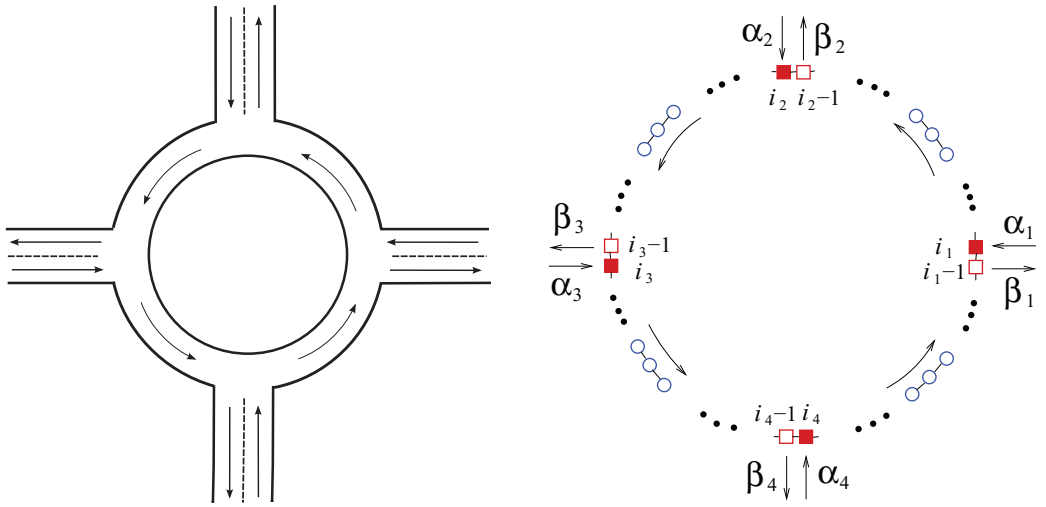

FIG. 1. Illustration of a single lane roundabout with $S = 4$ intersecting streets (left graph) and its representation (right graph) by sites in the model. The blue circles represent the sites along the interior lane of the roundabout, and the filled and open red squares represent the entrance and exit sites i_s and $i_s - 1$, $s = 1, \ldots 4$, of the interacting streets, respectively. Cars are attempting to enter the roundabout with the rate α_s from street s at site i_s. Cars with destination to the street s are exiting the roundabout with rate β_s at site $i_s - 1$.

II. MODEL FOR A SINGLE-LANE ROUNDABOUT

We consider the roundabout to consist of one interior circulating lane that is connected to a number of S streets, as illustrated in Fig. 1. The circulating lane is divided into L sites, where each site $i = 1, \ldots, L$ can be occupied by at most one car. The motion of the cars proceeds counterclockwise. It is described by the TASEP with sequential update, i.e., by stochastic unidirectional displacements to vacant nearest neighbor site with an attempt rate γ, where we set $\gamma^{-1} = 1$ as the time unit. To avoid onerous case distinctions, the site indices i are allowed to have values outside the range $1, \ldots, L$ in the following, corresponding to a periodic continuation of the indexing. A value i outside the range then refers to $(i \mod L) + 1$.

At an intersection with a street s, cars are attempting to enter the interior lane with rate α_s and they can exit it with rate β_s, where

$$0 < \alpha_s, \beta_s \leqslant \gamma \equiv 1. \tag{1}$$

The entering to and exiting from street s takes place at the entrance site i_s and the preceding exit site $i_s - 1$ of the circulating lane in clockwise direction (see Fig. 1). The corresponding intersections are arranged in ascending order, i.e., $i_s < i_{s+1}$. Between two intersection sites, there is at least one interior lane site without connection to a street, which implies $(i_{s+1} - i_s) \geqslant 3$. As for the site indices, we agree on a periodic continuation of the street indexing, i.e., a street index outside the range $1, \ldots, S$ refers to $(s \mod S) + 1$.

Cars entering the interior lane have a certain exit destination. This is described by a route matrix W_{rs}, where W_{rs} gives the probability that a car leaves the roundabout at street s under the condition that it entered it from street r. Any car entering the roundabout must leave it, i.e., the columns of the route matrix are normalized to one,

$$\sum_{s=1}^{S} W_{rs} = 1. \tag{2}$$

Repeated circulations of cars along the roundabout are disregarded, which means that a car can pass at most $L - 1$ sites along the roundabout. In this case it exits at the same street from which it came. The route matrix introduces a coupling between the TASEP in the interior lane sections between consecutive intersecting streets. These interior lane sections will be referred to as "substreets" in the following.

In general, the coupling between substreets will not solely be determined by the route matrix, but also by the properties of the junctions of the intersecting streets with the interior lane. In case of vehicular traffic, a car should not enter the roundabout, if another "conflicting car" approaches the respective entrance site along the circulating lane. To incorporate this effect in the model, we do not allow an entering of the roundabout from street s, if the site $i_s - 1$ preceding the entrance site i_s is occupied by a car that intends to continue to move along the circulating lane. This is the least restrictive possibility for including the conflicting car effect. Alternative ways would be to allow cars to enter at site i_s only if site $i_s - 1$ is empty, or by requiring a number of consecutive sites preceding the entrance site to be empty.

A. Kinetic equations

To describe the microstates and dynamics of the model in mathematical terms, we denote a car that enters the roundabout at street r and exits it at street s as an (r,s) car, and introduce the site occupation numbers,

$$n_i^{rs} = \begin{cases} 1, & \text{if site } i \text{ is occupied by an } (r,s) \text{ car,} \\ 0, & \text{otherwise.} \end{cases} \tag{3}$$

The notation n_i^{rs} is used here as a convenient abbreviation for $n_i^{(r,s)}$. Because at most one car can occupy a site, it holds $n_i^{rs} n_j^{r's'} = n_i^{rs} \delta_{ij} \delta_{rr'} \delta_{ss'}$, and the exclusion of repeated circulations implies that $n_i^{rs} = 0$ for all sites lying between the entrance site i_s of street s and the exit point $i_r - 1$ of street r in counterclockwise direction (see Fig. 1 [56]). The possible

sets $\{n_i^{rs}\}$ of occupation numbers specify the microstates of the roundabout model.

The dynamics of the model are governed by a master equation, which gives the time evolution of the microstate probabilities $p(\{n_i^{rs}\},t)$. With the route matrix and the rates for the enter and exit processes, as well as the displacement processes along the circulating lane specified, the explicit form of the master equation and rate equations of observables can be obtained by employing the general methods described in Ref. [57].

Here the time evolution and steady-state profiles of the average occupation numbers, $\rho_i^{rs}(t) = \langle n_i^{rs}(t)\rangle$, henceforth referred to as "densities," are of interest, where $\langle\ldots\rangle$ means an average over $p(\{n_i^{rs}\},t)$. For interior lane sites i ($i \neq i_s - 1$ and $i \neq i_s$, $s = 1,\ldots S$), the corresponding rate equations are

$$\frac{d\rho_i^{rs}}{dt} = j_{i-1}^{rs} - j_i^{rs}, \tag{4}$$

where

$$j_i^{rs} = \left\langle n_{i-1}^{rs}(1-n_i)\right\rangle \tag{5}$$

is the current of (r,s) cars from site $(i-1)$ to site i, and

$$n_i = \sum_{r,s=1}^{S} n_i^{rs} \tag{6}$$

is the total occupation number at site i irrespective of the car type. The current j_{i-1}^{rs} in Eq. (4) describes the gain of (r,s) cars due to transitions from site $i-1$ to site i, which are only possible if site $i-1$ is occupied by an (r,s) car and if site i is empty [factors n_{i-1}^{rs} and $(1-n_i)$ in $\langle n_{i-1}^{rs}(1-n_i)\rangle$ of Eq. (5)]. The current j_i^{rs} in Eq. (4) describes the corresponding loss term due to transitions from site i to site $i+1$.

For exit sites ($i = i_s - 1$, $s = 1,\ldots,S$) the rate equations are

$$\frac{d\rho_{i_s-1}^{qr}}{dt} = \begin{cases} j_{i_s-2}^{qs} - j_{\rm out}^{qs}, & r = s, \\ j_{i_s-2}^{qr} - j_{i_s-1}^{qr}, & r \neq s. \end{cases} \tag{7}$$

For $r \neq s$ the dynamics are the same as for interior lane sites. If $r = s$, however, we have to take into account that the (q,s) cars exit to street s, which is described by the outflow current,

$$j_{\rm out}^{qs} = \beta_s \rho_{i_s-1}^{qs}. \tag{8}$$

At entrance sites ($i = i_s$, $s = 1,\ldots,S$) we have

$$\frac{d\rho_{i_s}^{qr}}{dt} = \begin{cases} j_{\rm in}^{sr} - j_{i_s}^{sr}, & q = s, \\ j_{i_s-1}^{qr} - j_{i_s}^{qr}, & q \neq s. \end{cases} \tag{9}$$

Here the interior lane dynamics hold for $q \neq s$. For $q = s$ we must take into account the inflow of (s,r) cars from street s. This is given by

$$j_{\rm in}^{sr} = \alpha_s W_{sr}\left\langle\left(1 - n_{i_s-1}^{\rm cf}\right)(1-n_{i_s})\right\rangle, \tag{10}$$

where

$$n_{i_s-1}^{\rm cf} = \sum_{q=s+1}^{s+S-1}\sum_{r=s+1}^{q} n_{i_s-1}^{qr} \tag{11}$$

is the occupation number of "conflicting cars" at site $i_s - 1$.

Equation (10) has the following interpretation: Cars are trying to enter street s with a rate α_s, and the probability that a car is of (s,r) type is given by W_{sr}. An entering of a car is only possible if site i_s is empty and if there is no conflicting car at site $i_s - 1$ [factors $(1-n_{i_s})$ and $(1-n_{i_s-1}^{\rm cf})$ in $\langle(1-n_{i_s-1}^{\rm cf})(1-n_{i_s})\rangle$]. The conflicting car occupation number in Eq. (11) can be easily understood by considering the first street $s = 1$, where $n_{i_1-1}^{\rm cf} = \sum_{q=2}^{S}\sum_{r=2}^{q} n_{i_1-1}^{qr}$: From the cars entering the roundabout from street $q = 2$, only the ones exiting to the same street $r = 2$ pass the first street; cf. also Fig. 1. From the cars entering from street $q = 3$, the ones exiting to streets $r = 2$ or $r = 3$ pass the first street. Accordingly, from the cars entering from street q ($q = 2,\ldots,S$), the ones exiting to streets $r = 2,\ldots,q$ pass street $s = 1$. With our modulo convention for the street indices, this generalizes to Eq. (11) for the other streets $s = 2,\ldots,S$.

To arrive at a closed set of rate equations for the ρ_i^{rs}, the correlations between occupation numbers ("density correlations") appearing in Eqs. (5) and (10) need to be expressed in terms of the densities. The simplest way is to use the mean-field approximation (MFA), where correlations are neglected, which means that averages over products of occupation numbers are factorized. With respect to our focus on determining phases of car densities between intersecting streets in the stationary state, this MFA is expected to give good results, like it gives for the standard TASEP. More advanced methods, as, e.g., the time-dependent density functional theory for lattice fluids [58] and the Markov chain approach to kinetics [59], become particularly relevant, if interactions beyond site exclusion are considered.

B. Stationary states and throughput of cars

In the stationary state of the roundabout, the time derivatives in Eqs. (4), (7), and (9) are zero, which implies a balancing of the respective currents. Each substreet between two consecutive intersecting streets of the interior lane then is characterized by a stationary car density profile, which reflects one of the possible phases of the standard TASEP [54,55], i.e., either the low-density (LD) phase, the high-density (HD) phase, or the maximum current (MC) phase. To determine the occurrence of these phases in dependence of the sets $\{\alpha_s\}$, $\{\beta_s\}$, and $\{W_{rs}\}$ of model parameters, we will use the MFA and first express the partial densities at the exit sites as functions of the total densities at the entrance sites. Then we employ an effective rate approach, which connects the known phases of the standard TASEP with the phases of the substreets. This concept of effective rates was earlier introduced to treat isolated "defects" in the TASEP [60] and, analogously as in this work, successfully applied to identify stationary nonequilbrium phases in a TASEP chain containing a splitting into two lanes in its interior [61].

One may ask whether a description based on the TASEP density profiles is appropriate for application to vehicular traffic, because in this case typical roundabouts are not large, while the TASEP phases are characterized by a nearly flat bulk density, which forms in the interior of the substreets sufficiently distant from the junctions with the intersecting streets. One can give a positive answer to this question with some restrictions. In the LD and HD phases the density profiles

decay exponentially towards the bulk regime, with additional power law factors in subphases [55]. The respective correlation length is on the order of the lattice constant except for a small region around the transition lines of the LD and HD phases to the MC phase. Hence for identifying the LD and HD phases in the substreets, their size in general can be small. For the MC phase, the density profile decays slowly as a power law towards the bulk. However, for small system sizes, the profile has an inflection point close to the point where the density passes the value $1/2$, which reflects the limiting bulk density in an infinite system. Hence, also the MC phase can be well identified and distinguished from the LD and HD phases even if the substreet lengths are small. Practically, one can consider the densities in the middle of the substreets as the order parameter of the phases for small roundabouts, as we will show below in Sec. III D.

In the following Sec. III we first demonstrate the general procedure outlined above for $S=2$ streets and test the results against kinetic Monte Carlo (KMC) simulations of the roundabout dynamics. Then we show in Sec. IV how the method generalizes to roundabouts with an arbitrary number of intersecting streets. We give the essential details of this generalization and show some results for $S=3$ and $S=4$.

As it turns out, only the exit and entrance sites are relevant in the treatment. It is thus helpful to use an abbreviated and more transparent notation for the densities at the exit and entrance sites of street s:

$$\rho_s^{qr} \equiv \rho_{i_s-1}^{qr} \quad : \text{partial densities at exit site,}$$

$$\rho_s^{\mathrm{cf}} \equiv \sum_{q=s+1}^{s+S-1} \sum_{r=s+1}^{q} \rho_{i_s-1}^{qr} \quad : \text{conflicting car density at exit site,}$$

$$\rho_s^{\mathrm{out}} \equiv \sum_{r=1}^{S} \rho_{i_s-1}^{rs} \quad : \text{density of cars leaving at exit site,}$$

$$\rho_s^{\mathrm{ex}} \equiv \rho_s^{\mathrm{cf}} + \rho_s^{\mathrm{out}} \quad : \text{density at exit site,}$$

$$\rho_s^{\mathrm{ent}} \equiv \sum_{q,r=1}^{S} \rho_{i_s}^{qr} \quad : \text{density at entrance site.}$$

Similarly, in addition to j_{out}^{sr} and j_{in}^{sr} defined in Eqs. (8) and (10), we introduce the currents for the inflow and outflow of cars at street s, and the currents for cars passing street s:

$$j_s^{\mathrm{out}} \equiv \beta_s \rho_s^{\mathrm{out}} \quad : \text{outflow current of cars,}$$

$$j_s^{\mathrm{in}} \equiv \sum_{r=1}^{S} j_{\mathrm{in}}^{sr} \quad : \text{inflow current of cars,}$$

$$j_s^{qr} \equiv j_{i_s}^{qr} \quad : \text{current of passing } (q,r) \text{ cars, } q=s+1,\ldots,s+S-1,\ r=s+1,\ldots,q$$

$$j_s^{\mathrm{pass}} \equiv \sum_{q=s+1}^{s+S-1} \sum_{r=s+1}^{q} j_s^{qr} \quad : \text{current of all passing cars.}$$

Note that $j_s^{\mathrm{in}} = \alpha_s \langle (1-n_{i_s-1}^{\mathrm{cf}})(1-n_{i_s})\rangle_0$ and $j_s^{\mathrm{pass}} = \langle n_{i_s-1}^{\mathrm{cf}}(1-n_{i_s})\rangle_0$, where the average $\langle\ldots\rangle_0$ refers to the stationary state.

In the stationary state, the correlations defining the currents at the entrance and exit sites, as well as the set $\{\rho_s^{\mathrm{out}}\}$, can be expressed exactly in terms of the $\{\rho_s^{\mathrm{ent}}\}$ and the model parameters without resorting to the MFA. This is shown in Appendix. For calculating the phases via the concept of the effective rates, however, we also need the $\{\rho_s^{\mathrm{cf}}\}$ as a function of the $\{\rho_s^{\mathrm{ent}}\}$, which will become clear below. This requires some type of mean-field treatment. This observation agrees with the earlier finding [61] that the balancing of currents alone is not sufficient for determining effective rates at junctions of TASEP chains. Knowing j_s^{pass}, the $\{\rho_s^{\mathrm{cf}}\}$ can be calculated from the approximation $\rho_s^{\mathrm{cf}} \simeq j_s^{\mathrm{pass}}/(1-\rho_s^{\mathrm{ent}})$, which leads to an alternative mean-field approach, where only $\langle n_{i_s-1}^{\mathrm{cf}}(1-n_{i_s})\rangle_0$ is factorized (see Appendix).

In the MFA all correlations are factorized. The expressions for the currents can then be summarized as

$$j_{\mathrm{out}}^{rs} = \beta_s \rho_s^{rs}, \tag{12a}$$

$$j_s^{\mathrm{out}} = \beta_s \rho_s^{\mathrm{out}}, \tag{12b}$$

$$j_{\mathrm{in}}^{sr} = \alpha_s W_{sr}\big(1-\rho_s^{\mathrm{cf}}\big)\big(1-\rho_s^{\mathrm{ent}}\big), \tag{12c}$$

$$j_s^{\mathrm{in}} = \alpha_s\big(1-\rho_s^{\mathrm{cf}}\big)\big(1-\rho_s^{\mathrm{ent}}\big), \tag{12d}$$

$$j_s^{qr} = \rho_s^{qr}\big(1-\rho_s^{\mathrm{ent}}\big), \tag{12e}$$

$$j_s^{\mathrm{pass}} = \rho_s^{\mathrm{cf}}\big(1-\rho_s^{\mathrm{ent}}\big), \tag{12f}$$

where Eq. (12e) applies for $q=s+1\ldots,s+S-1$ and $r=s+1,\ldots,q$.

The throughput of cars in a stationary state is given by the total inflow J_{in} or outflow of J_{out} of cars:

$$J^{\mathrm{in}} = \sum_{s=1}^{S} j_s^{\mathrm{in}} = \sum_{s=1}^{S} j_s^{\mathrm{out}} = J^{\mathrm{out}}. \tag{13}$$

Maximizing this throughput with respect to the model parameters, which control the traffic, e.g., the sets $\{\alpha_s\}$ and $\{\beta_s\}$ of injection and ejection rates, gives the conditions of optimal transport.

III. ROUNDABOUT WITH TWO STREETS

A. Partial densities at exit sites as functions of total densities at entrance sites

For two streets, there are six partial densities at the exit sites: ρ_1^{11}, ρ_1^{21}, ρ_1^{22}, ρ_2^{22}, ρ_2^{12}, and ρ_2^{11}. To express them as a function of the two densities ρ_1^{ent} and ρ_2^{ent} at the entrance sites, we utilize the fact that in the stationary state the inflow current j_{in}^{11} of $(1,1)$ cars must equal the current j_2^{11} of $(1,1)$ cars passing the second street and the outflow current j_{out}^{11} of $(1,1)$ cars, i.e., $j_{\mathrm{in}}^{11} = j_2^{11} = j_{\mathrm{out}}^{11}$. Moreover, it must hold $j_{\mathrm{in}}^{12} = j_{\mathrm{out}}^{12}$ for the $(1,2)$ cars, and analogously $j_{\mathrm{in}}^{22} = j_1^{22} = j_{\mathrm{out}}^{22}$ and $j_{\mathrm{in}}^{21} = j_{\mathrm{out}}^{21}$ for cars entering from the second street.

Accordingly, with Eqs. (12a), (12c), and (12e) we obtain from the balancing of the currents for the different types of cars at the intersecting streets ($\rho_1^{\mathrm{cf}} = \rho_1^{22}$ and $\rho_2^{\mathrm{cf}} = \rho_2^{11}$ here for $S=2$):

$$\alpha_1 W_{11}\big(1-\rho_1^{22}\big)\big(1-\rho_1^{\mathrm{ent}}\big) = \rho_2^{11}\big(1-\rho_2^{\mathrm{ent}}\big) = \beta_1\rho_1^{11}, \tag{14a}$$

$$\alpha_1 W_{12}\big(1-\rho_1^{22}\big)\big(1-\rho_1^{\mathrm{ent}}\big) = \beta_2\rho_2^{12}, \tag{14b}$$

$$\alpha_2 W_{22}\big(1-\rho_2^{11}\big)\big(1-\rho_2^{\mathrm{ent}}\big) = \rho_1^{22}\big(1-\rho_1^{\mathrm{ent}}\big) = \beta_2\rho_2^{22}, \tag{14c}$$

$$\alpha_2 W_{21}\big(1-\rho_2^{11}\big)\big(1-\rho_2^{\mathrm{ent}}\big) = \beta_1\rho_1^{21}. \tag{14d}$$

These are six linear equations, which can be solved to express the six partial densities in terms of the densities at the entrance sites and the model parameters. Note that, due to symmetry, Eqs. (14c) and (14d) follow from Eqs. (14a) and (14b) by a shifting of the street indices by one, which according to the modulo convention here is equivalent to interchanging the street indices 1 and 2. The solutions read

$$\rho_1^{11} = \frac{\alpha_1 W_{11}\left[\left(1-\rho_1^{\mathrm{ent}}\right) - \alpha_2 W_{22}\left(1-\rho_2^{\mathrm{ent}}\right)\right]}{\beta_1(1-\alpha_1 W_{11}\alpha_2 W_{22})}, \tag{15a}$$

$$\rho_1^{21} = \frac{\alpha_2 W_{21}\left[\left(1-\rho_2^{\mathrm{ent}}\right) - \alpha_1 W_{11}\left(1-\rho_1^{\mathrm{ent}}\right)\right]}{\beta_1(1-\alpha_1 W_{11}\alpha_2 W_{22})}, \tag{15b}$$

$$\rho_1^{22} = \frac{\alpha_2 W_{22}\left[\left(1-\rho_2^{\mathrm{ent}}\right) - \alpha_1 W_{11}\left(1-\rho_1^{\mathrm{ent}}\right)\right]}{\left(1-\rho_1^{\mathrm{ent}}\right)\left(1-\alpha_1 W_{11}\alpha_2 W_{22}\right)}, \tag{15c}$$

for the first street, and for the second street are obtained by index interchanging.

B. Splitting of roundabout into substreets

Analogous to earlier treatments of defects [60] or double-chain sections [61] in the TASEP, we split the roundabout into two TASEP substreets with effective inflow and outflow rates. The substreet s refers to the interior lane part between the intersecting streets s and $s+1$. For $S=2$ this means that the first substreet is entered at site i_1 with effective rate $\tilde{\alpha}_1$, and exited at site i_2-1 with rate $\tilde{\beta}_1$, while the second substreet is entered at site i_2 with effective rate $\tilde{\alpha}_2$, and exited at site i_1-1 with rate $\tilde{\beta}_2$. Hence we obtain for the effective in- and outflow currents of the substreets:

$$\tilde{j}_s^{\mathrm{in}} = \tilde{\alpha}_s\left(1-\rho_s^{\mathrm{ent}}\right), \tag{16a}$$

$$\tilde{j}_s^{\mathrm{out}} = \tilde{\beta}_s \rho_{s+1}^{\mathrm{ex}}. \tag{16b}$$

The effective rates are fixed by requiring that these total in- and outflow currents of cars at the respective entrance and exit sites are the same as in the roundabout.

The total inflow (outflow) currents to (from) the entrance (exit) sites in the roundabout are given by the sums of the respective total currents of entering and exiting and passing cars [see Eqs. (12b), (12d), and (12f)]:

$$j_s^{\mathrm{in}} + j_s^{\mathrm{pass}} = \left[\alpha_s\left(1-\rho_s^{\mathrm{cf}}\right) + \rho_s^{\mathrm{cf}}\right]\left(1-\rho_s^{\mathrm{ent}}\right), \tag{17a}$$

$$\begin{aligned} j_s^{\mathrm{out}} + j_s^{\mathrm{pass}} &= \beta_s \rho_s^{\mathrm{out}} + \rho_s^{\mathrm{cf}}\left(1-\rho_s^{\mathrm{ent}}\right) \\ &= \beta_s\left(\rho_s^{\mathrm{ex}} - \rho_s^{\mathrm{cf}}\right) + \rho_s^{\mathrm{cf}}\left(1-\rho_s^{\mathrm{ent}}\right). \end{aligned} \tag{17b}$$

In fact, because of car number conservation, it must hold $j_s^{\mathrm{in}} + j_s^{\mathrm{pass}} = j_{s+1}^{\mathrm{out}} + j_{s+1}^{\mathrm{pass}}$, which can be readily proven from the balancing of the partial currents discussed in Sec. III A. Setting

$$\tilde{j}_s^{\mathrm{in}} = j_s^{\mathrm{in}} + j_s^{\mathrm{pass}} = j_{s+1}^{\mathrm{out}} + j_{s+1}^{\mathrm{pass}} = \tilde{j}_s^{\mathrm{out}}, \tag{18}$$

we can write the determining equations for the effective rates in the form ($s=1,2$),

$$\tilde{\alpha}_s = \alpha_s\left(1-\rho_s^{\mathrm{cf}}\right) + \rho_s^{\mathrm{cf}}, \tag{19a}$$

$$\tilde{\beta}_s \rho_{s+1}^{\mathrm{ex}} = \tilde{\alpha}_s\left(1-\rho_s^{\mathrm{ent}}\right). \tag{19b}$$

The second equation is also required by consistency, because for a TASEP in the stationary state, the inflow and outflow current must be the same. Equation (19) gives the effective rates in terms of the densities $\{\rho_s^{\mathrm{ent}}\}$ and the model parameters.

We note in passing that, differently from what one may think when looking at Eq. (10) [or Eq. (15)], the parameters α_s and W_{sr} are entering the effective rates not only in the combination $\alpha_s W_{sr}$. This reflects the fact that a coupling between the substreets is mediated by the route matrix via the conditions implied on the partial occupation numbers and by the conflicting car constraint as discussed in Sec. II.

C. Phase diagram for roundabout

In each of the substreets, either the LD, MC, or HD phase of the TASEP can form. Hence there are in total nine phases possible (LD/LD, LD/MC, LD/HD, MC/LD, ...). With respect to the roundabout, these phases μ (μ = LD, MC or HD) characterize the car densities in the interior ("bulk") parts of the substreets. In the language of phase transitions, the bulk densities serve as order parameters.

Which phases appear for given model parameters depends on the values of the effective rates. For an ordinary TASEP with injection rate $\tilde{\alpha}$ and ejection rate $\tilde{\beta}$, the following properties are known [55]:

LD phase: occurs for $0 \leqslant \tilde{\alpha} < 1/2$, $\tilde{\alpha} < \tilde{\beta}$, and the bulk density is $\rho_{\mathrm{LD}} = \tilde{\alpha}$.

MC phase: occurs for $\tilde{\alpha} > 1/2$, $\tilde{\beta} > 1/2$, and the bulk density is $\rho_{\mathrm{MC}} = 1/2$.

HD phase: occurs for $0 \leqslant \tilde{\beta} < 1/2$, $\tilde{\alpha} > \tilde{\beta}$, and the bulk density is $\rho_{\mathrm{HD}} = 1-\tilde{\beta}$.

For $\tilde{\alpha} = \tilde{\beta} < 1/2$, the LD and HD phase coexist.

We encode these conditions for the occurrence of the different TASEP phases by defining the logical functions,

$$\mathrm{Cond}_\mu(\tilde{\alpha},\tilde{\beta}) = \begin{cases} 0 \leqslant \tilde{\alpha} < \frac{1}{2} \wedge \tilde{\beta} > \tilde{\alpha}\,, & \mu = \mathrm{LD}, \\ \tilde{\alpha} > \frac{1}{2} \wedge \tilde{\beta} > \frac{1}{2}, & \mu = \mathrm{MC}, \\ 0 \leqslant \tilde{\beta} < \frac{1}{2} \wedge \tilde{\alpha} > \tilde{\beta}, & \mu = \mathrm{HD}, \end{cases} \tag{20}$$

where $\wedge$ denotes the Boolean AND operator. The bulk densities in the different TASEP phases are specified by

$$\rho_\mu^{\mathrm{TASEP}}(\tilde{\alpha},\tilde{\beta}) = \begin{cases} \tilde{\alpha}\,, & \mu = \mathrm{LD}, \\ \frac{1}{2}\,, & \mu = \mathrm{MC}, \\ 1-\tilde{\beta}\,, & \mu = \mathrm{HD}, \end{cases} \tag{21}$$

and the respective stationary currents by

$$J_\mu^{\mathrm{TASEP}}(\tilde{\alpha},\tilde{\beta}) = \rho_\mu^{\mathrm{TASEP}}\left(1-\rho_\mu^{\mathrm{TASEP}}\right). \tag{22}$$

In the phase μ of the TASEP, the inflow current $\tilde{\alpha}(1-\rho^{\mathrm{ent}})$ to the entrance site is equal to $J_\mu^{\mathrm{TASEP}}(\tilde{\alpha},\tilde{\beta})$, yielding $\rho^{\mathrm{ent}} = 1 - J_\mu^{\mathrm{TASEP}}(\tilde{\alpha},\tilde{\beta})/\tilde{\alpha}$ for the density at the entrance site [55].

Accordingly, one can identify a multiphase μ_1/μ_2 for the roundabout by the following procedure. In the phase μ_1/μ_2, the densities at the entrance sites must be

$$\rho_{s,\mu_s}^{\mathrm{ent}} = 1 - \frac{J_{\mu_s}^{\mathrm{TASEP}}(\tilde{\alpha}_s,\tilde{\beta}_s)}{\tilde{\alpha}_s}. \tag{23}$$

Inserting these densities for ρ_s^{ent} in Eqs. (19a) and (19b) (note that ρ_s^{cf} and ρ_{s+1}^{ex} depend on ρ_s^{ent}), we obtain a set of (in

general nonlinear) equations, from which the effective rates $\tilde{\alpha}_s$, $\tilde{\beta}_s$ are calculated as functions of the model parameters. The μ_1/μ_2 phase occurs, if $\tilde{\alpha}_s$ and $\tilde{\beta}_s$ satisfy the conditions for the corresponding phases. This means that the μ_1/μ_2 phase forms if

$$\mathrm{Cond}_{\mu_1}(\tilde{\alpha}_1,\tilde{\beta}_1) \wedge \mathrm{Cond}_{\mu_2}(\tilde{\alpha}_2,\tilde{\beta}_2) = .\mathrm{True}. \tag{24}$$

The region (set) of corresponding control parameters satisfying Eq. (24), is denoted as $\mathcal{R}_{\mu_1/\mu_2}$. The car densities in the interior parts of the substreets in phase μ_1/μ_2 are

$$\rho^{\mathrm{lane}}_{s,\mu_s} = \rho^{\mathrm{TASEP}}_{\mu_s}(\tilde{\alpha}_s,\tilde{\beta}_s). \tag{25}$$

If $\tilde{\alpha}_s = \tilde{\beta}_s < 1/2$, the car density in the substreets is not unique, but two coexisting regions of the LD and HD phase appear with densities $\rho^{\mathrm{lane}}_s = \tilde{\alpha}_s$ and $\rho^{\mathrm{lane}}_s = 1-\tilde{\beta}_s$, respectively.

Applying this procedure for all possible phases, one can map out the complete phase diagram in the parameter space. This phase diagram is not exact, because of the approximations associated with the mean-field treatment of correlations and with the effective rate method in Sec. III B. In view of previous results on TASEP models, we expect deviations to the true phase diagram to be small. This expectation is indeed corroborated by results from KMC simulations shown below.

Because $\tilde{\alpha}_s$ and $\tilde{\beta}_s$ depend on the model parameters, ρ^{lane}_s varies with these parameters if substreet s is in the LD or HD phase. In this respect the behavior here of the "interacting TASEP" is similar to the TASEP behavior in the presence of particle interactions beyond site exclusion [59,62], or in connection with periodic driving [63].

The throughput from Eq. (13) in phase μ_1/μ_2 can most conveniently be calculated from the solutions for $\rho^{\mathrm{out}}_{s,\mu_s}$, which are given by the respective partial densities (see Sec. II B) after inserting Eq. (23) into Eq. (15):

$$J^{\mathrm{out}}_{\mu_1/\mu_2} = \sum_{s=1}^{S} \beta_s \rho^{\mathrm{out}}_{s,\mu_s} = \sum_{r,s=1}^{S} \beta_s \rho^{rs}_{s,\mu_s}. \tag{26}$$

Maximal throughput $J^{\mathrm{out,max}}_{\mu_1/\mu_2}$ in phase μ_1/μ_2 is obtained for those control parameter values (e.g., $\{\alpha_s\}$ and $\{\beta_s\}$ in region $\mathcal{R}_{\mu_1,\mu_2}$), where $J^{\mathrm{out}}_{\mu_1/\mu_2}$ becomes maximal, and the parameter sets for optimal throughput follow by comparison of the $J^{\mathrm{out,max}}_{\mu_1/\mu_2}$.

D. Results for equivalent intersecting streets

For equivalent intersecting streets with equal values of corresponding parameters, we can write

$$w \equiv W_{11} = W_{22}, \quad W_{12} = W_{21} = 1-w, \tag{27a}$$

$$\alpha \equiv \alpha_1 = \alpha_2, \tag{27b}$$

$$\beta \equiv \beta_1 = \beta_2. \tag{27c}$$

As a consequence, it must hold $\rho_2^{11} = \rho_1^{22}, \rho_2^{12} = \rho_1^{21}, \rho_2^{22} = \rho_1^{11}$, and $\rho_2^{\mathrm{ent}} = \rho_1^{\mathrm{ent}} \equiv \rho^{\mathrm{ent}}$. Equation (15) becomes

$$\rho_1^{11} = \frac{\alpha w}{\beta(1+\alpha w)}(1-\rho^{\mathrm{ent}}), \tag{28a}$$

$$\rho_1^{21} = \frac{\alpha(1-w)}{\beta(1+\alpha w)}(1-\rho^{\mathrm{ent}}), \tag{28b}$$

$$\rho_1^{22} = \frac{\alpha w}{1+\alpha w}. \tag{28c}$$

Accordingly we obtain for $\rho^{\mathrm{cf}} \equiv \rho_1^{\mathrm{cf}} = \rho_2^{\mathrm{cf}} = \rho_1^{22}$ and $\rho^{\mathrm{ex}} \equiv \rho_1^{\mathrm{ex}} = \rho_2^{\mathrm{ex}} = \rho_1^{11} + \rho_1^{21} + \rho_1^{22}$:

$$\rho^{\mathrm{cf}} = \frac{\alpha w}{1+\alpha w}, \tag{29}$$

$$\rho^{\mathrm{ex}} = \frac{\alpha(1-\rho^{\mathrm{ent}}+\beta w)}{\beta(1+\alpha w)}. \tag{30}$$

Inserting these expressions into Eqs. (19a) and (19b) and solving for the effective rates yields

$$\tilde{\alpha} = \frac{\alpha(1+w)}{1+\alpha w}, \tag{31a}$$

$$\tilde{\beta} = \frac{\beta(1+w)(1-\rho^{\mathrm{ent}})}{1-\rho^{\mathrm{ent}}+\beta w}. \tag{31b}$$

For the equivalent streets considered here, $\tilde{\alpha}$ turns out to be independent of ρ^{ent}.

In this symmetric case, only the LD/LD, MC/MC, and HD/HD phases can appear. To determine their occurrence, we insert $\rho^{\mathrm{ent}} = 1 - J_\mu(\tilde{\alpha},\tilde{\beta})/\tilde{\alpha}$ from Eq. (23) for $\mu = $ LD, MC, and HD into Eq. (31b), solve for $\tilde{\beta}$ (necessary here only for the HD/HD phase), and determine the model parameter values α, β, and w, where $\mathrm{Cond}_\mu(\tilde{\alpha},\tilde{\beta})$ is satisfied.

For the LD/LD phase we obtain

$$\tilde{\beta} = \frac{\beta(1-\alpha)(1+w)}{1-\alpha+\beta w+\alpha\beta w^2}, \tag{32}$$

and the parameter region $\mathcal{R}_{\mathrm{LD/LD}}$,

$$0 \leqslant \alpha < \frac{1}{2+w} \wedge \frac{\alpha(1-\alpha)}{1-\alpha-\alpha^2 w(1+w)} < \beta \leqslant 1. \tag{33}$$

For the MC/MC phase we find

$$\tilde{\beta} = \frac{\beta(1+w)(1+\alpha w)}{1+\alpha w+4\alpha\beta w(1+w)}, \tag{34}$$

and the parameter region $\mathcal{R}_{\mathrm{MC/MC}}$,

$$\frac{1}{2+w} < \alpha \leqslant \begin{cases} 1, & 0 \leqslant w \leqslant \frac{1}{2}, \\ \frac{1+2w}{w(3+2w)}, & w \geqslant \frac{1}{2}, \end{cases} \wedge \frac{(1+\alpha w)}{2[1+w-\alpha w(1+w)]} < \beta \leqslant 1. \tag{35}$$

For the HD/HD phase, Eq. (31b) has three different solutions, including the trivial one $\tilde{\beta} = 0$. The physical branch of the remaining two solutions (containing a root) can be selected from the requirement that $\tilde{\beta} = \beta$ for $w \to 0$ (no coupling between the two streets). This gives

$$\tilde{\beta} = \frac{1}{2(1+\alpha w)}(1+\beta+(\alpha+\beta)w+\alpha\beta w(1+w) - \sqrt{(1+\alpha w)[(1+\alpha w)(1+\beta+\beta w)^2 - 4\beta(1+w)]}). \tag{36}$$

The parameter region $\mathcal{R}_{\mathrm{HD/HD}}$ is the part of the α-β square $0 \leqslant \alpha,\beta \leqslant 1$ that is not covered by the LD/LD or MC/MC

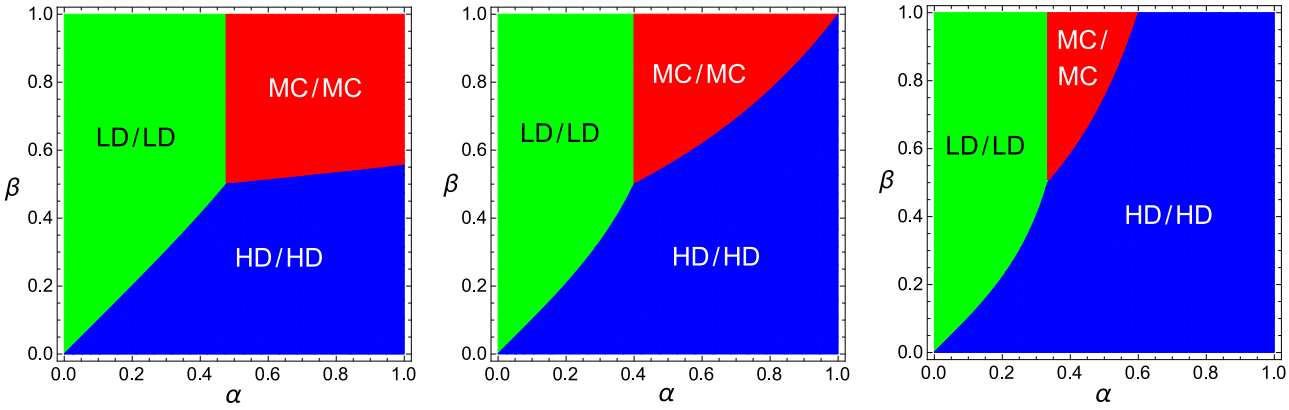

FIG. 2. Phase diagram for a roundabout with $S = 2$ equivalent streets having equal entrance and exit rates α and β, for $w = 0.1$ (left panel), 0.5 (middle panel), and 1 (right panel).

phases (and excluding the transition lines). On the transition line between the LD/LD and HD/HD phases, i.e., for

$$\beta = \frac{\alpha(1-\alpha)}{1-\alpha-\alpha^2 w(1+w)}, \quad 0 \leqslant \alpha < \frac{1}{2+w}, \tag{37}$$

the LD and HD phases coexist in each of the two substreets. We note that the coexistence in both substreets implies a rapid change of the local density close to the junctions.

Figure 2 shows the phase diagram of the symmetric roundabout for three values of w, which gives the strength of the substreet coupling mediated by the route matrix. For $w = 0.1$, the coupling is weak and the phase diagram looks almost as the one for the standard TASEP, which is recovered in the limit $w \to 0$ (for each substreet). With increasing w, the HD/HD phase grows, while the LD/LD and MC/MC phases shrink. The second-order transition line between the MC/MC and HD/HD phase becomes rounded and appears to rotate counterclockwise. For $w < 0.5$ it terminates at the right boundary of the α-β square, hits its upper right corner for $w = 0.5$, and terminates at the upper boundary for $w > 0.5$. This means that the roundabout for $w > 0.5$ can be in the HD/HD phase for all values of β if α is large. The first-order transition line between the LD/LD and HD/HD phases becomes also rounded with increasing w. Its terminus is the triple point in the middle of the diagram, which moves slightly to the left with increasing w. The second-order line between the LD/LD and MC/MC phases, by contrast, remains straight independent of w, and shifts towards the left with the triple point.

Overall, the main effect of increasing the coupling strength w is an extension of the HD/HD phase, going along with a strong shrinkage of the MC/MC phase and a squeezing of the LD/LD phase to the upper left of the α-β square. The extension of the HD/HD phase results from the fact that the number of cars passing the intersections becomes higher with larger w, and accordingly $\tilde{\alpha}$ increases and $\tilde{\beta}$ decreases. As a consequence, the state of the roundabout is driven to the HD/HD phase with increasing w.

As mentioned above, the phase diagrams in Fig. 2 are not exact because of the neglect of correlations in the mean-field treatment and the use of the effective rate method. To test the quality of these approximations, we performed KMC simulations for roundabouts of different lengths L and with entrance sites of the intersecting streets at $i_1 = 1$ and $i_2 = L/2 + 1$. These simulations were carried out with the reaction-time algorithm [64,65]. Figure 3 shows representative density profiles in the LD/LD, MC/MC, and HD/HD phase for $L = 200$, and for $w = 0.5$, where the mean-field phase diagram is shown in the middle panel of Fig. 2. Because of the equivalence of the two intersecting streets, the stationary density profiles exhibit the symmetry $\rho_i = \rho_{i+L/2}$. At the junction with the intersecting streets, the profiles show a rapid jumplike change from a small value at the exit sites to a higher value at the entrance sites, see the behavior at the sites $i = 100$ and $i = 101$. A corresponding behavior occurs at the sites $i = L$ and $i = 1$.

Different from the behavior in the LD phases of the (standard) ASEP, the profile in the LD/LD is not flat at the "left ends" of the two substreets (i.e., for $\rho_{1+j} = \rho_{L/2+1+j}$ with $j = 0, 1, \ldots$ small). It rather decreases monotonically towards the flat bulk regime. Analogously, the profile in the HD/HD is not flat at the "right ends" of the two substreets (i.e., for

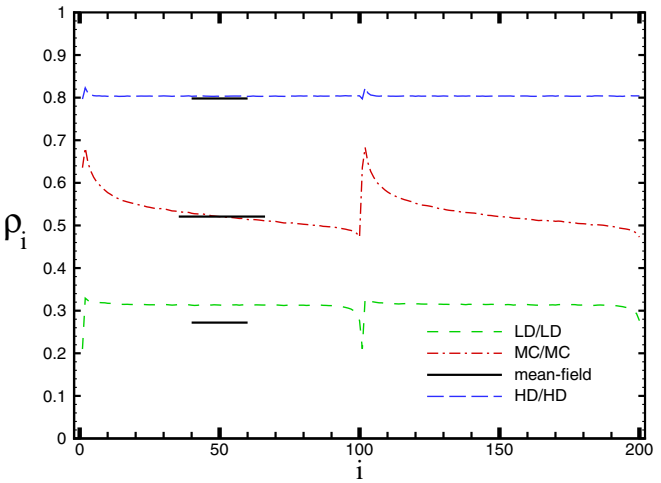

FIG. 3. Simulated density profiles in a roundabout with $S = 2$ equivalent streets for $w = 0.5$ in the LD/LD ($\alpha = 0.2$, $\beta = 0.8$), MC/MC ($\alpha = 0.6$, $\beta = 0.7$), and HD/HD phase ($\alpha = 0.7$, $\beta = 0.2$). Bulk densities predicted by the mean-field theory are indicated by the black horizontal lines.

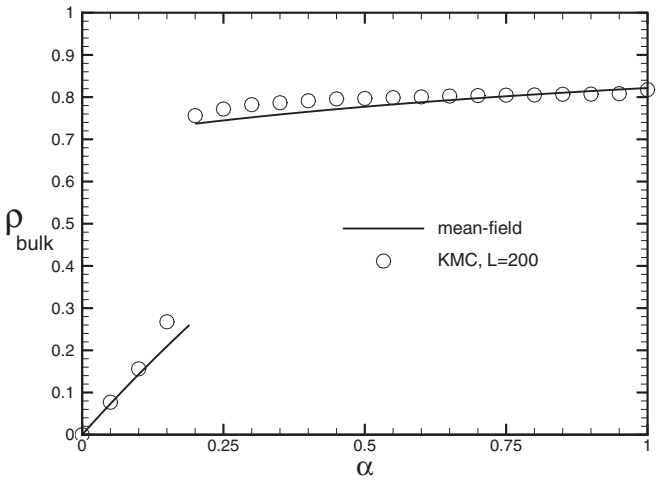

FIG. 4. Bulk density as a function of α in a roundabout with $S = 2$ equivalent streets for fixed $\beta = 0.2$ and $w = 0.5$. Results from the KMC simulations (symbols) for a roundabout of length $L = 200$ are compared with the prediction of the mean-field treatment (solid line).

$\rho_{L-j} = \rho_{L/2-j}$ with $j = 0, 1, \ldots$ small). The deviations from a flat form are caused by the fact that the dynamics at the junctions is modified compared to the one in the bulk (interior of the substreets) [59,63]. Overall we found the bulk densities predicted by the mean-field treatment to be in fair agreement with the simulated values. For the profiles shown in Fig. 3, the predicted bulk density (small horizontal lines) agrees well with the simulated value for the HD/HD phase (and for the MC/MC phase, where it is equal to one-half), while it is slightly smaller than the simulated one in the LD/LD phase.

Figure 4 shows the simulated bulk density (symbols) as a function of α in comparison with the mean-field prediction for $\beta = 0.2$ and $w = 0.5$ fixed. According to Eq. (33), the LD/LD phase appears for small α up to a value $\alpha_\times$, which is given by $\alpha_\times(1-\alpha_\times)/[1-\alpha_\times-\alpha_\times^2 w(1+w)] = \beta$, and for $w = 0.5$

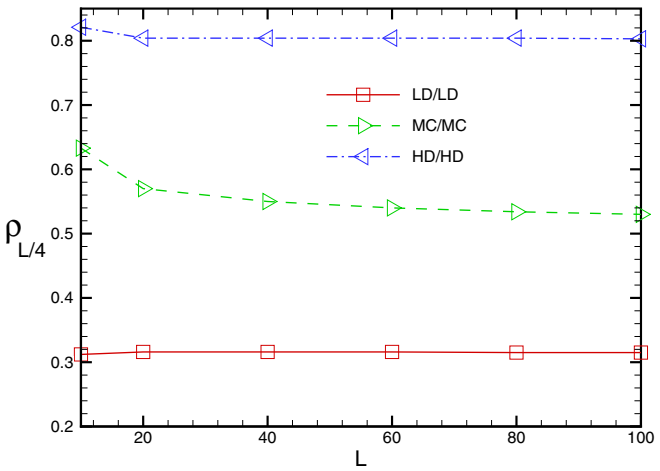

FIG. 5. Midpoint density at site $i = \frac{L}{4}$ versus roundabout length L. Streets have equal entrance and exit rates α and β. Entrance and exits rates α and β, and the route matrix parameter w are the same as in Fig. 3.

and $\beta = 0.2$ yields $\alpha_\times \simeq 0.193$. For $\alpha > \alpha_\times$, the HD/HD is predicted to appear [see Fig. 2 (middle panel)]. Indeed, close to $\alpha_\times$, we see a corresponding jump in the simulated data for the bulk density in Fig. 4.

Simulations of smaller roundabouts show comparable density profiles down to values of about $L \simeq 20$, which demonstrates that the theory can be useful also for typical roundabouts in vehicular traffic. In Fig. 5 we show the density in the middle of the substreets, i.e. at sites $i = L/4$ (or $i = 3L/4$), as a function of L. As can be seen from the figure, these midpoint densities are almost independent of L in the LD/LD and HD/HD phases for $L \gtrsim 20$, and in the MC/MC phase there is only a weak increase with decreasing L. Let us note that the time for reaching a stationary state becomes small also for small L.

E. Results for nonequivalent intersecting streets

For nonequivalent intersecting streets, the substreets of the interior lane can be in different TASEP phases, and in total nine phases μ_1/μ_2 can appear in the roundabout. In this more general case, it becomes difficult to solve Eqs. (19a) and (19b) for the effective rates and the conditions (24) for identifying the correct phases analytically and we found it easier to resort to numerical solutions.

As an example, let us consider varying injection rates α_1 and α_2 for fixed $W_{11} = W_{22} = 0.5$ and $\beta_1 = \beta_2 = 0.6$. The resulting phase diagram in the α_1-α_2 square $0 \leqslant \alpha_1, \alpha_2 \leqslant 1$, displayed in Fig. 6, shows the occurrence of seven different phases. Along the diagonal $\alpha_1 = \alpha_2$, we recover the LD/LD, MC/MC, and HD/HD phases from Fig. 2 for $w = 0.5$ (middle panel), corresponding to the horizontal line in this graph for $\beta = 0.6$. With respect to the diagonal, the diagram in Fig. 6 is symmetric in the sense that the phases μ_1 and μ_2 of the

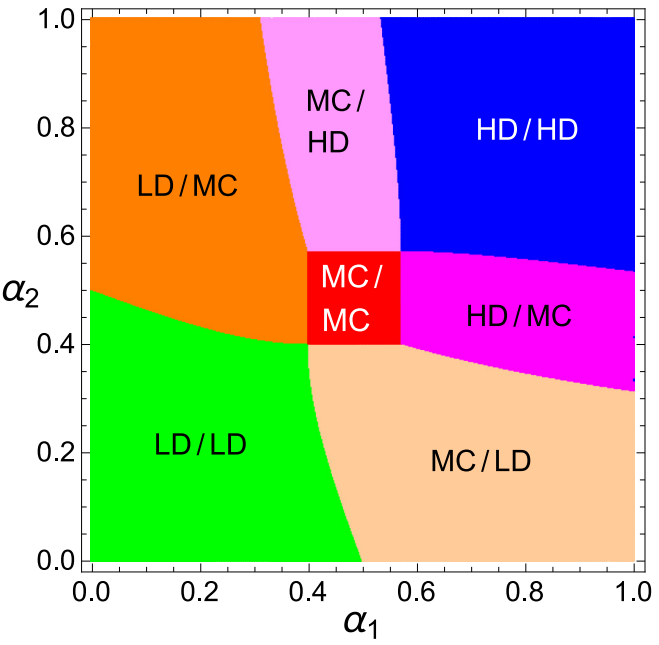

FIG. 6. Phase diagram for $S = 2$ streets in dependence of the entrance rates α_1 and α_2. The exit rates are fixed to $\beta_1 = \beta_2 = 0.6$ and the independent route matrix elements to $W_{11} = W_{22} = 0.5$.

two substreets interchange if α_1 and α_2 are interchanged. This is because the route matrix elements and the exit rates are equal for the two intersecting streets. Considering the upper left half $\alpha_2 \geqslant \alpha_1$ of the diagram, the appearance of the mixed phases with $\mu_1 \neq \mu_2$ can be understood from the fact that with larger α_2, the effective injection rate to the second substreet increases and, accordingly the phase μ_2 of this substreet is driven towards the MC and HD phase. Hence the LD/LD phase changes into the LD/MC phase and the MC/MC phase into the MC/HD phase when following lines at fixed α_1 upwards from the diagonal.

IV. ROUNDABOUTS WITH $S > 2$ STREETS

The treatment in the preceding section can be generalized to an arbitrary number S of intersecting streets. The first step is to determine the partial densities at the exit sites as functions of the total densities at the entrance sites. There are $S^2(S+1)/2$ nonzero partial densities ρ_s^{qr} in general. This can be seen by considering the first street $s = 1$, where $\rho_1^{qr} = 0$ for $q < r$. Accordingly, the number of nonzero $\rho_1^{qr}, q \geqslant r$, is $S(S+1)/2$. Because this number s the same for each intersecting street, in total $S^2(S+1)/2$ partial densities need to be calculated.

Following the procedure outlined in Sec. III A, the balancing of the currents of cars entering at the first street and exiting to streets $1, S, S-1, \ldots, 2$ yields

$$j_{\text{in}}^{11} = j_2^{11} = \ldots = j_{S-1}^{11} = j_S^{11} = j_{\text{out}}^{11}, \quad [S \text{ eqs.}] \tag{38a}$$

$$j_{\text{in}}^{1S} = j_2^{1S} = \ldots = j_{S-1}^{1S} = j_{\text{out}}^{1S}, \quad [(S-1) \text{ eqs.}] \tag{38b}$$

$$\vdots$$

$$j_{\text{in}}^{13} = j_2^{13} = j_{\text{out}}^{13}, \quad [2 \text{ eqs.}] \tag{38c}$$

$$j_{\text{in}}^{12} = j_{\text{out}}^{12}. \quad [1 \text{ eq.}] \tag{38d}$$

These are $\sum_{j=1}^{S} j = S(S+1)/2$ equations. For the other streets $s = 2, \ldots, S$, the corresponding equations for the current balancing follow by street index shifting. After inserting the MFA expressions for the currents from Eq. (12), we thus have a set of $S^2(S+1)/2$ linear equations for the partial densities at the exit sites, which can be solved to express them in terms of the total densities $\rho_s^{\text{ent}}, s = 1, \ldots, S$, at the entrance sites. As mentioned in Sec. II B, Eq. (38) can be used also to calculate all correlations $\langle n_{i_s-1}^{qr} n_i \rangle_0$ and all ρ_s^{out} as functions of the $\{\rho_s^{\text{ent}}\}$ and model parameters without using the MFA (see Appendix).

The remaining steps are fully analogous to the procedure described in Secs. III B and III C. To test whether, for a given set of model parameters, the multiphase $\mu_1/\mu_2/\ldots/\mu_S$ appears in the roundabout, corresponding to the TASEP phases $\mu_s, s = 1, \ldots, S$, in the substreets, the effective rates $\tilde{\alpha}_s, \tilde{\beta}_s$ are calculated from Eq. (19). To this end the $\rho_{s,\mu_s}^{\text{ent}}$ from Eq. (23) are inserted into the respective expressions for the partial densities, which appear in Eq. (19). If the so-calculated effective rates satisfy

$$\bigwedge_{s=1}^{S} \text{Cond}_{\mu_s}(\tilde{\alpha}_s, \tilde{\beta}_s) = .\text{True.}, \tag{39}$$

the phase $\mu_1/\mu_2/\ldots/\mu_S$ can form. The optimal throughput follows from maximizing the current in Eq. (26).

It should be noted here that it cannot be ruled out *a priori* that Eq. (39) [or Eq. (24)] are fulfilled by two (or more) different multiphases for a region of model parameters, which does not constitute a submanifold (i.e., transition line, or, more generally speaking, phase transition submanifold in model parameter space). In the numerical solutions, as well as in our analytical treatments, however, we always found that for a given set of values $\{\alpha_s\}$, $\{\beta_s\}$, $\{W_{rs}\}$ outside the transition submanifolds, exactly one multiphase $\mu_1/\ldots/\mu_S$ was satisfying the condition (39). This suggests that the additional consideration of noise in the model will not be of crucial importance in the sense that the noise becomes decisive for selecting a stable stationary state from multiple solutions.

With the general scheme given above, phase diagrams and control parameter sets for optimal throughput can be calculated numerically, for nonequivalent intersecting streets, as was demonstrated for the case $S = 2$ in Sec. III E. For S streets, in total 3^S different multiphases are possible. In the special case of equivalent intersecting streets, only three of these multiphases can appear, where all substreets are either in the LD, MC, or HD TASEP phase. In the following section we show that in this case the problem for $S > 2$ intersecting streets can be reduced to the one treated analytically in Sec. III D for $S = 2$ after replacing the coupling strength w with a generalized expression.

A. Reduction to case $S = 2$ for $S > 2$ equivalent intersecting streets

Let us define $\alpha \equiv \alpha_1 = \ldots \alpha_S$, $\beta \equiv \beta_1 = \ldots \beta_S$, and the route matrix elements as

$$W_{11} = W_{22} = W_{33} = \ldots = W_{SS} \equiv w_1, \tag{40a}$$

$$W_{1S} = W_{21} = W_{32} = \ldots = W_{S,S-1} \equiv w_2, \tag{40b}$$

$$W_{1,S-1} = W_{2S} = W_{31} = \ldots = W_{S,S-2} \equiv w_3, \tag{40c}$$

$$\vdots$$

$$W_{13} = \ldots = W_{S-2,S} = W_{S-1,1} = W_{S,2} \equiv w_{S-1}, \tag{40d}$$

$$W_{12} = W_{23} = \ldots = W_{S-1,S} = W_{S,1} \equiv \bar{w}, \tag{40e}$$

where

$$\bar{w} \equiv 1 - \sum_{j=1}^{S-1} w_j \tag{41}$$

follows from the normalization condition (2) [66]. Note that we introduced the route matrix elements $\mathbf{w} = (w_1, \ldots, w_{S-1})$ in a way that for $\mathbf{w} \to 0$, the interior lane of the roundabout splits into independent substreets. After inserting Eq. (12) into Eq. (38), and when taking into account that the ρ_s^{ent}, $\rho_{s+j}^{q+j,r+j}$, $s, j = 1, \ldots, S$, must all be the same for equivalent intersecting streets, we can set $\rho^{\text{ent}} \equiv \rho_s^{\text{ent}}$, $\rho^{qr} \equiv \rho_{s+j}^{q+j,r+j}$,

and write Eq. (38) in the following form:

$$\alpha w_1(1-\rho^{\mathrm{cf}}) = \rho^{SS} = \rho^{S-1,S-1} = \ldots = \rho^{22} = \beta\frac{\rho^{11}}{1-\rho^{\mathrm{ent}}}, \tag{42a}$$

$$\alpha w_2(1-\rho^{\mathrm{cf}}) = \rho^{S,S-1} = \rho^{S-1,S-2} = \ldots = \rho^{32} = \beta\frac{\rho^{21}}{1-\rho^{\mathrm{ent}}}, \tag{42b}$$

$$\alpha w_3(1-\rho^{\mathrm{cf}}) = \rho^{S,S-2} = \rho^{S-1,S-3} = \ldots = \rho^{42} = \beta\frac{\rho^{31}}{1-\rho^{\mathrm{ent}}}, \tag{42c}$$

$$\vdots$$

$$\alpha w_{S-1}(1-\rho^{\mathrm{cf}}) = \rho^{S,2} = \beta\frac{\rho^{S-1,1}}{1-\rho^{\mathrm{ent}}}, \tag{42d}$$

$$\alpha \bar{w}(1-\rho^{\mathrm{cf}}) = \beta\frac{\rho^{S,1}}{1-\rho^{\mathrm{ent}}}. \tag{42e}$$

Here $\rho^{\mathrm{cf}} = \sum_{q=2}^{S}\sum_{r=2}^{q}\rho^{qr} = \rho^{22} + \rho^{32} + \rho^{33} + \ldots + \rho^{S,2} + \ldots + \rho^{SS}$ (see Sec. II B). We see that the ρ^{qr} with $r \neq 1$ in Eqs. (42a)–(42d) sum up to ρ^{cf}. Combining the corresponding summation with the leftmost terms $\alpha w_j(1-\rho^{\mathrm{cf}})$ in Eqs. (42a)–(42d), a closed equation for ρ^{cf} is obtained, whose solution gives Eq. (29) with the generalized coupling strength,

$$w \equiv \sum_{j=1}^{S-1}(S-j)w_j. \tag{43}$$

For $S = 2$, this coupling strength reduces to $w = W_{11} = W_{22}$. The weighting of the w_j with $(S-j)$ in Eq. (43) can be intuitively understood from the fact that the w_j, as defined in Eq. (42), involve the passing of $(S-j)$ consecutive intersecting streets by cars, i.e., a coupling of $(S-j)$ substreets.

Summing up the rightmost terms $\beta\rho^{j,1}/(1-\rho^{\mathrm{ent}})$, $j = 1,\ldots,S$, in Eqs. (42a)–(42e) and combining this summation with the leftmost terms $\alpha w_j(1-\rho^{\mathrm{cf}})$ in Eqs. (42a)–(42d), as well as $\alpha\bar{w}(1-\rho^{\mathrm{cf}})$ in Eq. (42e), we furthermore find

$$\rho^{\mathrm{out}} = \sum_{j=1}^{S}\rho^{j1} = \frac{\alpha(1-\rho^{\mathrm{ent}})}{\beta(1+\alpha w)}. \tag{44}$$

For $\rho^{\mathrm{ex}} = \rho^{\mathrm{cf}} + \rho^{\mathrm{out}}$ (cf. Sec. II B) we hence recover Eq. (30) with w from Eq. (43). This completes the derivation which shows that the $S > 2$ case reduces to the $S = 2$ case.

For $S = 2$ the coupling strength w is bounded by one, $0 \leqslant w \leqslant 1$. Because of the weighting of the w_j in Eq. (43), this is no longer true for $S > 2$ and the range of possible values changes to $0 \leqslant w \leqslant (S-1)$. This does not affect the general solutions for the phases given in Eqs. (33) and (34). However, the shrinkage of the LD/. . ./LD and MC/. . ./MC phases with increasing w, as discussed for the graphs shown in Fig. 2, persists for w exceeding one. Their extension as a function of w can be quantified by the crossing of the respective phase transition curves with the $\beta = 1$ line. The intersection of the transition curve between the LD/. . ./LD and MC/. . ./MC phases and the $\beta = 1$ line is given by $\alpha_{\mathrm{LD/MC}} = 1/(2+w)$ [see Eq. (33)], yielding an α interval $[0,\alpha_{\mathrm{LD/MC}}]$ for the appearance of the LD/. . ./LD phase. The intersection of the transition curve between the MC/. . ./MC and HD/. . ./HD phases and the $\beta = 1$ line is given by $\alpha_{\mathrm{MC/HD}} = (1+2w)/[w(3+2w)]$ [see Eq. (35)], yielding an α interval $[\alpha_{\mathrm{LD/MC}},\alpha_{\mathrm{MC/HD}}]$ for the appearance of the MC/. . ./MC phase. Accordingly, the respective α interval for the LD/. . ./LD phase shrinks as $\sim w^{-1}$ for large w, and the α interval for the MC/. . ./MC phase more rapidly with $\sim w^{-2}$. This implies also that the occurrence of the MC/. . ./MC phase becomes less likely with increasing number of intersecting streets.

V. SUMMARY AND PERSPECTIVES

We have studied a model for traffic in a roundabout, where the dynamics along the roundabout's interior lane are described by the TASEP. The overall stationary transport behavior in the roundabout could by classified by the TASEP phases of car densities appearing in substreets, which constitute the parts of the interior lane between consecutive intersecting streets. The car flows in the substreets become coupled via a modified dynamics at the junctions with the intersecting streets, and via a route matrix, which accounts for the given entrance and exit points of cars to the roundabout. In the stationary state of a roundabout with S intersecting streets, 3^S different multiphases can appear, which correspond to the possible TASEP phases in the S substreets.

Based on a mean-field treatment and an effective rate concept for substreet decoupling, we developed a general scheme for calculating the multiphases for an arbitrary number S of intersecting streets with arbitrary entrance and exit rates as well as route matrix elements. With these phases determined, it becomes possible to calculate parameter sets for optimal throughput of cars in the roundabout. In general, the solutions of the equations for the effective rates and the determination of the phases have to be found numerically. For equivalent intersecting streets with equal parameters, analytical solutions could be obtained, and the general behavior for S intersecting streets can be derived from the solution for two equivalent intersecting streets. In this special case, only three multiphases are possible by symmetry, where all substreets are in the same TASEP phase.

Previous results for the TASEP suggest that our mean-field treatment can be expected to give a good approximation to the exact solution with respect to the phase structure. This expectation was indeed confirmed by KMC simulations for a roundabout with three intersecting streets. An alternative MFA variant is discussed in Appendix.

From a general point of view, the methodology of our treatment of the roundabout model should be useful also for other systems, where collective transport in elementary parts of a system can be modeled by the TASEP or variants of it, and where these elementary parts become coupled by intersections or crossings. This opens up the possibility to describe and understand stationary states of collective nonlinear dynamics in traffic networks.

With respect to vehicular traffic, it would be interesting to see, whether the multiphases in the roundabout and their shifting with varying control parameters occur also in more

realistic models, for example, when modeling the car dynamics along the interior lane by the TASEP with simultaneous update, or when resorting to nonlinear continuum descriptions. We believe that the essential features described in this work remain valid on a qualitative level, but this conjecture needs to be checked in the future. For practical applications, further studies based on more detailed models may allow one also to derive guidelines for controlling, which in the simplified approach of this work are reflected in the rates for entering (exiting) the interior lane from (to) the intersecting streets. Effectively, these rates correspond to a reduced flow of cars at the junctions, which could be steered, e.g., by traffic lights.

ACKNOWLEDGMENTS

M.E.F. would like to thank the Osnabrück University for kind hospitality and support during two visits, where major parts of this work were carried out. We are grateful to Azadeh Saeidi for technical support in preparing the manuscript.

APPENDIX: ALTERNATIVE MEAN-FIELD TREATMENT

To avoid the factorization of correlations in the first step of the general treatment, one can express the stationary inflow currents as

$$\begin{aligned} j_{\text{in}}^{sr} &= \alpha_s W_{sr} \left\langle \left(1 - n_{i_s-1}^{\text{cf}}\right)\left(1 - n_{i_s}\right)\right\rangle_0 \\ &= \alpha_s W_{sr} \left(1 - \rho_s^{\text{ent}} - j_s^{\text{pass}}\right), \end{aligned} \tag{A1}$$

where $j_s^{\text{pass}} = \sum_{q=s+1}^{s+S-1} \sum_{r=s+1}^{q} j_s^{qr}$ (cf. Sec. II B) and

$$j_s^{qr} = \left\langle n_{i_s-1}^{qr}\left(1 - n_{i_s}\right)\right\rangle_0, \tag{A2}$$

are the partial currents of passing cars at the intersections, which equal correlations of the occupancies at the exit and entrance sites.

As discussed above, the current balancing in (38), including its extension to the other streets $s = 2, \ldots, S$ obtained by street index shifting, gives a set of $S^2(S+1)$ equations. This can be regarded as a linear system for solving the $S^2(S-1)/2$ partial currents j_s^{qr} $(q = (s+1), \ldots, s+S-1,\ r = s+1, \ldots, q,$ $s = 1, \ldots, S)$ and the S^2 partial densities ρ_s^{qs} $(q, s = 1, \ldots, S)$ of leaving cars at the exit sites [entering the $j_{\text{out}}^{qs} = \beta_s \rho_s^{qs}$ in Eq. (38)] in terms of the densities ρ_s^{ent} $(s = 1, \ldots, S)$ at the entrance sites (and the model parameters).

Let us now consider the j_s^{qr} and ρ_s^{qs} as the solutions of this system. Then one can proceed as discussed in Sec. III B and identify the TASEP current for the effective inflow currents $\tilde{j}_s^{\text{in}} = \tilde{\alpha}_s(1 - \rho_s^{\text{ent}})$ from Eq. (16a) with the real total inflow currents,

$$\begin{aligned} j_s^{\text{in}} &= \sum_{r=1}^{S} j_{\text{in}}^{sr} = \alpha_s \left(1 - \rho_s^{\text{ent}} - j_s^{\text{pass}}\right) \\ &= \alpha_s \left(1 - \rho_s^{\text{ent}} - \sum_{q=s+1}^{s+S-1} \sum_{r=s+1}^{q} j_s^{qr}\right). \end{aligned} \tag{A3}$$

This gives

$$\tilde{\alpha}_s \left(1 - \rho_s^{\text{ent}}\right) = \alpha_s \left(1 - \rho_s^{\text{ent}} - \sum_{q=s+1}^{s+S-1} \sum_{r=s+1}^{q} j_s^{qr}\right) \tag{A4}$$

as determining equations for the effective rates $\tilde{\alpha}_s$, which replace Eq. (19a).

Because of car number conservation (see the discussion in Sec. III B), the determining equations (19b) for the effective rates $\tilde{\beta}_s$ remain unchanged:

$$\begin{aligned} \tilde{\beta}_s \rho_{s+1}^{\text{ex}} &= \tilde{\beta}_s \left(\rho_{s+1}^{\text{cf}} + \rho_{s+1}^{\text{out}}\right) \\ &= \tilde{\beta}_s \left(\rho_{s+1}^{\text{cf}} + \sum_{q=1}^{S} \rho_{s+1}^{q,s+1}\right) = \tilde{\alpha}_s \left(1 - \rho_s^{\text{ent}}\right). \end{aligned} \tag{A5}$$

Up to this point, correlation functions have not been factorized, but Eq. (A5) contains the densities ρ_s^{cf} of passing cars at the exit sites, which are not known from the solution of the current balancing equations (38). One can extract ρ_s^{cf} from a factorization of the correlations in $j_s^{\text{pass}} = \langle n_{i_s-1}^{\text{cf}} n_{i_s} \rangle_0$, yielding

$$\rho_{s+1}^{\text{cf}} \simeq \frac{j_{s+1}^{\text{pass}}}{1 - \rho_{s+1}^{\text{ent}}} \tag{A6}$$

as an alternative MFA. After inserting this into Eq. (A5), the phase diagrams and optimal throughput can be determined as described in the main text.

[1] A. Schadschneider, D. Chowdhury, and K. Nishinari, in *Stochastic Transport in Complex Systems: From Molecules to Vehicles*, 1st ed. (Elsevier Science, Amsterdam, 2010), Chap. 5.
[2] E. Brockfeld, R. Barlovic, A. Schadschneider, and M. Schreckenberg, Phys. Rev. E **64**, 056132 (2001).
[3] M. E. Fouladvand, M. R. Shaebani, and Z. Sadjadi, J. Phys. Soc. Jpn. **73**, 3209 (2004).
[4] D.-W. Huang and W.-N. Huang, Physica A **370**, 747 (2006).
[5] C. Gershenson, Ph.D thesis, Virje Universiteit Brussel, Brussels, 2002.
[6] N. Moussa, Int. J. Mod. Phys. C **18**, 1047 (2007).
[7] S. Lämmer and D. Helbing, J. Stat. Mech. (2008) P04019.
[8] D. Helbing and A. Mazloumian, Eur. Phys. J. B **70**, 257 (2009).
[9] A. C. Soh, M. Khalid, M. H. Marhaban, and R. Yusof, Simulation Modelling Practice and Theory **17**, 1081 (2009).
[10] M. Li, Z.-J. Ding, R. Jiang, M.-B. Hu, and B.-H. Wang, J. Stat. Mech. (2011) P12001.
[11] J. de Gier, T. M. Garoni, and O. Rojas, J. Stat. Mech. (2011) P04008.
[12] D. Zubillaga, G. Cruz, L. D. Aguilar, J. Zapotécatl, N. Fernandez, J. Aguilar, and C. Gershenson, Entropy **16**, 2384 (2014).
[13] M. E. Fouladvand and M. Nematollahi, Eur. Phys. J. B **22**, 395 (2001).

[14] D.-W. Huang and W.-N. Huang, Phys. Rev. E **67**, 056124 (2003).
[15] D.-W. Huang and W.-N. Huang, Int. J. Mod. Phys. C **14**, 539 (2003).
[16] M. E. Fouladvand, Z. Sadjadi, and M. R. Shaebani, J. Phys. A: Math. Gen. **37**, 561 (2004).
[17] S. Belbasi and M. E. Foulaadvand, J. Stat. Mech. (2008) P07021.
[18] M. Krbalek, J. Phys. A: Math. Theor. **41**, 205004 (2008).
[19] A. Varas, M. D. Cornejo, B. A. Toledo, V. Mūnoz, J. Rogan, R. Zarama, and J. A. Valdivia, Phys. Rev. E **80**, 056108 (2009).
[20] M. Fukui, K. Nishinari, Y. Yokoya, and Y. Ishibashi, Phyisica A **388**, 1207 (2009).
[21] Z. J. Ding, X. Y. Sun, R. R. Liu, Q. M. Wang, and B. H. Wang, Int. J. Mod. Phys. C **21**, 443 (2010).
[22] D.-W. Huang, Int. J. Mod. Phys. C **21**, 189 (2010).
[23] R. Oertel and P. Wagner, *Transportation Research Board 90th Annual Meeting*, Report No. 11-1719 (Transportation Research Board, Washington, DC, 2011).
[24] C. Appert-Rolland, J. Cividini, and H. J. Hilhorst, J. Stat. Mech. (2011) P10014.
[25] H.-D. He, W.-Z. Lu, and L.-Y. Dong, Chin. Phys. B **20**, 040514 (2011).
[26] Q.-L. Li, R. Jiang, B.-H. Wang, and M.-R. Liu, Int. J. Mod. Phys. C **23**, 1250068 (2012).
[27] A. Mhirech and A. A. Ismaili, Int. J. Mod. Phys. C **24**, 1350050 (2013).
[28] P. Radhakrishnan and T. V. Mathew, J. Comp. Civil Eng. **27**, 254 (2013).
[29] G. Abramson, V. Semeshenko, and J. R. Iglesias, PloS One **8**, e61876 (2013).
[30] P. Deo and H. J. Ruskin, Physica A **405**, 140 (2014).
[31] C.-J. Jin, W. Wang, R. Jiang, and H. Wang, Int. J. Mod. Phys. C **25**, 1350099 (2014).
[32] M. Krbalek and J. Sleis, J. Phys. A: Math. Theor. **48**, 015101 (2015).
[33] M. E. Foulaadvand and S. Belbasi, J. Phys. A: Math. Theor. **40**, 8289 (2007).
[34] X. G. Li, Z. Y. Gao, B. Jia, and X. M. Zhao, Int. J. Mod. Phys. C **20**, 501 (2009).
[35] D.-F. Xie, Z.-Y. Gao, X.-M. Zhao, and K.-P. Li, Physica A **388**, 2041 (2009).
[36] Q.-L. Li, R. Jiang, B.-H. Wang, and M.-R. Liu, Europhys. Lett. **99**, 38004 (2012).
[37] W. Zhang, W. Zhang, and W. Chen, Eur. Phys. J. B **85**, 78 (2012).
[38] H. Fan, B. Jia, J. Tian, and L. Yun, Physica A **415**, 172 (2014).
[39] C. J. Jin, W. Wang, and R. Jiang, Transportmetrica A: Transport Science **10**, 273 (2014).
[40] Q.-L. Li, R. Jiang, and B.-H. Wang, Physica A **419**, 349 (2015).
[41] R. Wang and H. J. Ruskin, Comp. Phys. Comm. **147**, 570 (2002).
[42] M. E. Fouladvand, Z. Sadjadi, and M. R. Shaebani, Phys. Rev. E **70**, 046132 (2004).
[43] B. Ray and S. N. Bhattacharyya, Phys. Rev. E **73**, 036101 (2006).
[44] R.-X. Chen, K.-Z. Bai, and M.-R. Liu, Chin. Phys. **15**, 1471 (2006).
[45] R. Wang and H. J. Ruskin, Int. J. Mod. Phys. C **17**, 693 (2006).
[46] D.-W. Huang, Physica A **383**, 603 (2007).
[47] C. Chang, Z. Fan, and Y. Sun, The UMAP Journal **30**, 227 (2009).
[48] K.-Z. Bai, H.-L. Tan, L.-J. Kong, and M.-R. Liu, Chin. Phys. B **19**, 040510 (2010).
[49] N. Lakouari, H. Ez-Zahraouy, and A. Benyoussef, Phys. Lett. A **378**, 3169 (2014).
[50] I. Zohdy and H. Rakha, Transport. Res. Rec.: J. Transport. Res. Board **2381**, 91 (2013).
[51] D.-W. Huang, Comp. Phys. Comm. **189**, 72 (2015).
[52] H. Echab, N. Lakuoari, H. Ez. Zahraouy, and A. Benyoussef, Int. J. Mod. Phys. C **27**, 1650009 (2016).
[53] H. Echab, N. Lakuoari, H. Ez. Zahraouy, and A. Benyoussef, Phys. Lett. A **380**, 992 (2016).
[54] B. Derrida, Phys. Rep. **301**, 65 (1998).
[55] G. Schütz, Phys. Rev. E **47**, 4265 (1993).
[56] With our modulo convention for the site indices, we can write this formally as $n_i^{rs} = 0$ for $r \neq s$ and $i = i_s + k$, $k = 0, \ldots, (i_r - i_s - 1) + K$, where $K = L$ for $r < s$ and zero otherwise.
[57] J.-F. Gouyet, M. Plapp, W. Dieterich, and P. Maass, Adv. Phys. **52**, 523 (2003).
[58] H. P. Fischer, J. Reinhard, W. Dieterich, J.-F. Gouyet, P. Maass, A. Majhofer, and D. Reinel, J. Chem. Phys. **108**, 3028 (1998).
[59] M. Dierl, M. Einax, and P. Maass, Phys. Rev. E **87**, 062126 (2013).
[60] A. B. Kolomeisky, J. Phys. A: Math. Gen. **31**, 1153 (1998).
[61] J. Brankov, N. Pesheva, and N. Bunzarova, Phys. Rev. E **69**, 066128 (2004).
[62] M. Dierl, P. Maass, and M. Einax, Phys. Rev. Lett. **108**, 060603 (2012).
[63] M. Dierl, W. Dieterich, M. Einax, and P. Maass, Phys. Rev. Lett. **112**, 150601 (2014).
[64] D. T. Gillespie, J. Comp. Phys. **28**, 395 (1978).
[65] V. Holubec, P. Chvosta, M. Einax, and P. Maass, Europhys. Lett. **93**, 40003 (2011).
[66] With our modulo convention, Eq. (40) may be written in compact form as $w_k = W_{j,j+1-k}$, $j = 1 \ldots, S$, $k = 1, \ldots, S-1$.